Journal of
Applied Crystallography
ISSN 0021-8898

Approximation of the structure factor for nonspherical hard bodies using polydisperse spheres

Steen Hansen

J. Appl. Cryst. (2013). **46**, 1008–1016

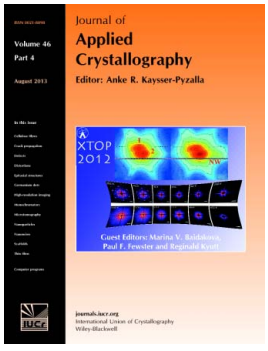

Journal of Applied Crystallography covers a wide range of crystallographic topics from the viewpoints of both techniques and theory. The journal presents papers on the application of crystallographic techniques and on the related apparatus and computer software. For many years, the *Journal of Applied Crystallography* has been the main vehicle for the publication of small-angle scattering papers and powder diffraction techniques. The journal is the primary place where crystallographic computer program information is published.

Journal of
Applied Crystallography
ISSN 0021-8898

Received 2 February 2013
Accepted 3 June 2013

Approximation of the structure factor for nonspherical hard bodies using polydisperse spheres

Steen Hansen

Niels Bohr Institute, University of Copenhagen, Universitetsparken 5, DK-2100 KBH Ø, Denmark. Correspondence e-mail: slh@nbi.dk

A new method for approximation of the structure factor for nonspherical hard bodies is suggested. It is shown that for moderate deviation from spherical symmetry the structure factor may be approximated by the structure factor for a size distribution of spheres. The distribution of spheres should be selected to give agreement between the excluded volume distance distribution functions for the two cases. As the excluded volume distance distribution may be calculated by Monte Carlo simulation for any particle and as a semi-analytical expression exists for the excluded volume distance distribution of a size distribution of spheres, it should be possible to apply the method to any shape of molecule. For ellipsoids of axial ratios between 0.5 and 2.0 a simple approximate expression is given for the parameters of the matching size distribution.

1. Introduction

Small-angle scattering is a technique that is often used for studying structures in solution (*e.g.* Glatter & Kratky, 1982; Feigin & Svergun, 1987). For analysis of small-angle scattering data with concentration effects it is necessary to include the structure factor in the analysis. However only a few analytical expressions for the structure factor exist [see the reviews by *e.g.* Pedersen (1997) or Svergun & Koch (2003), and references therein]. The structure factor for monodisperse hard spheres was given analytically by Percus & Yevick (1958), and Vrij (1979) extended the result to include polydisperse spheres.

Several approximations to the exact result of Vrij were made. The decoupling approximation by Kotlarchyk & Chen (1983) assumed that the size and position of two spheres were uncorrelated, which led to a very simple result. In the local monodisperse approximation Pedersen (1993) only included interactions between spheres of identical sizes. Both of these approximations led to significant deviations from the analytical result of Vrij, as a result of their unphysical assumptions. In the scaling approximation Gazzillo *et al.* (1999) included the sum of interacting radii and found a better estimate of the excluded volume of the spheres, which proved to be a good approximation to the analytical solution of Vrij (1979)

For deviation from spherical symmetry no analytical expressions exist for the structure factor. The most frequently used approximation for this case is that of the decoupling approximation which assumes that the position and orientation of the nonspherical particles are uncorrelated. However, as was the case for polydisperse spheres the decoupling approximation is likely to give wrong estimates, especially concerning the excluded volume of the particles. Recently Cohen *et al.* (2011) reported an even stronger correlation between position and orientation of ellipsoids of moderate axial ratios than theoretically predicted.

Below it is suggested that the structure factor for particles of moderate deviation from spherical symmetry may be approximated by the structure factor for a size distribution of spheres. It is well known that the form factor for a system of monodisperse ellipsoids is identical to the form factor for a size distribution of spheres (Mittelbach & Porod, 1962). This means that also the single-particle distance distribution functions for the two cases must be identical. Here it is suggested that the size distribution to be used for approximation of the structure factor is that which gives agreement between the excluded volume distance distributions of the two forms of scatterer. As the former may be calculated with good precision by Monte Carlo simulation (Hansen, 2012) and the latter is given by a semi-analytical expression using the results of Glatter (1980), it is in principle simple to determine the form of the relevant size distribution.

The method will be illustrated by a real space analysis of the case of polydisperse spheres, where the differences between the various approximations can be seen in their respective distance distribution functions. Using the results for polydisperse spheres it is shown that the problems of the decoupling approximation for nonspherical scatterers may in some cases be remedied by using a size distribution of spheres for calculation of the structure factor. For ellipsoids of moderate axial ratios a simple approximate expression is given for the parameters of the matching size distribution, allowing an easy calculation of the structure factor for this case.

2. Theory

2.1. Small-angle scattering

In small-angle scattering the intensity I is measured as a function of the length of the scattering vector $q = 4\pi \sin(\theta)/\lambda$,

where λ is the wavelength of the radiation and θ is half the scattering angle.

For scattering from a dilute solution of monodisperse particles of maximum dimension d, the intensity can be written as (see *e.g.* Glatter & Kratky, 1982, pp. 119–165)

$$I(q) = 4\pi n(\Delta\rho)^2 V \int_0^d p(r)\frac{\sin(qr)}{qr}\,\mathrm{d}r, \tag{1}$$

where n is the (average) number density of the particles, $\Delta\rho$ is the difference in scattering length density between the solute and the solvent, V is the volume of one particle, and $p(r)$ is the distance distribution function for the particle. In the following equations $\Delta\rho$ is set equal to unity.

2.2. Nondilute solutions

For nondilute solutions interactions between particles have to be included in the description.

The intensity can now be divided into a part that is due to intra-particle effects – the form factor $P(q)$ – and a part that is due to the remaining inter-particle effects – the structure factor $S(q)$. For spherical monodisperse particles

$$I(q) = nV^2 S(q)P(q). \tag{2}$$

For other cases $S(q)$ in equation (2) should be taken as an apparent structure factor.

For nondilute solutions the distance distribution function $p(r)$ may be replaced by a total distance distribution function $p_{\rm tot}(r)$ according to

$$I(q) = 4\pi n \int_0^\infty p_{\rm tot}(r)\frac{\sin(qr)}{qr}\,\mathrm{d}r, \tag{3}$$

where it should be noted that the explicit contribution from the volume V in equation (1) is now included in $p_{\rm tot}(r)$ as this will give a more convenient notation for the polydisperse case below. The total distance distribution function may be divided into terms depending on the interaction:

$$p_{\rm tot}(r) = p_1(r) - \eta p_{\rm excl}(r) + \eta p_{\rm struct}(r), \tag{4}$$

where η is the volume fraction ($\eta = nV$).

The single-particle distance distribution function is $p_1(r)$ and the concentration effects are expressed through $p_{\rm excl}(r)$, which is the distance distribution function of the excluded volume, and $p_{\rm struct}(r)$, which is the remaining part of the total distance distribution function referring to molecules outside the excluded volume. Thus $p_{\rm excl}(r)$ depends only on the geometrical shape of the molecule and is in principle quite easy to calculate, while $p_{\rm struct}(r)$ is more complicated as it depends on the interaction and the mutual arrangement of the molecules.

For monodisperse spheres Kruglov (2005) derived an analytical expression for the excluded volume distance distribution function.

Finally it may be noted that the first term on the right-hand side of equation (4) determines the form factor $P(q)$ when Fourier transformed according to equation (1), while all three terms in combination determine the structure factor $S(q)$.

2.3. The excluded volume for polydisperse spheres

Including polydispersity and introducing a normalized number distribution of radii $f(R)$, average values of parameters can be found by integration over $f(R)$. For example if the molecular volume $V(R) = 4/3\pi R^3$ the average $\langle V\rangle$ is given as

$$\langle V\rangle = \int_0^\infty f(R)V(R)\,\mathrm{d}R. \tag{5}$$

In the following, angular brackets denote the average with respect to the number distribution $f(R)$. In equation (4) the single-particle distance distribution function is now given by the weighted contribution from the spheres of different radii:

$$p_1(r) = \langle p_1(r,R)\rangle = \int_0^\infty p_1(r,R)f(R)\,\mathrm{d}R, \tag{6}$$

omitting brackets and explicit dependence upon R where appropriate. Using the definitions above,

$$\langle V^2\rangle = 4\pi\int_0^\infty p_1(r)\,\mathrm{d}r. \tag{7}$$

Glatter (1980) calculated the analytical expression for the cross-term distance distribution function $p_x(r, a, R_i, R_j)$ of two homogeneous spheres of radii R_i and R_j, separated by a distance a. From this the excluded volume distance distribution $p_{\rm excl}$ in equation (4) can be obtained by a weighted integration over the various distances between the centers of overlapping spheres as well as integrations over all combinations of the two specific sizes of the spheres according to

$$p_{\rm excl}(r) = \int_0^\infty f(R_j)\int_0^\infty f(R_i)\int_0^{R_i+R_j}(a^2/\langle V\rangle)p_x(r,a,R_i,R_j)\,\mathrm{d}a\,\mathrm{d}R_i\,\mathrm{d}R_j, \tag{8}$$

where

$$V_iV_j = 4\pi\int_0^{R_i+R_j+a} p_x(r,a,R_i,R_j)\,\mathrm{d}r. \tag{9}$$

As V_i and V_j are independent $\langle V_iV_j\rangle = \langle V\rangle^2$.

The reduced molecular volume $V_{\rm red}$ is given by

$$\begin{aligned} V_{\rm red} &= \langle V_{{\rm excl}\,i,j}\rangle/\langle V\rangle = \langle 4/3\pi(R_i+R_j)^3\rangle/\langle V\rangle \\ &= \int_0^\infty f(R_j)\int_0^\infty f(R_i)\int_0^{R_i+R_j}(4\pi a^2/\langle V\rangle)\,\mathrm{d}a\,\mathrm{d}R_i\,\mathrm{d}R_j, \end{aligned} \tag{10}$$

where $V_{{\rm excl}\,i,j,} = 4/3\pi(R_i+R_j)^3$ is the excluded volume for two spheres of radii R_i and R_j respectively.

The contribution to the forward scattering $I(0)$ from the excluded volume may be found from

$$4\pi\int_0^\infty p_{\rm excl}(r)\,\mathrm{d}r = \langle V_{{\rm excl}\,i,j}V_iV_j\rangle/\langle V\rangle. \tag{11}$$

2.4. The structure factor for nonspherical objects

The excluded volume distance distribution functions for any hard object may be calculated by Monte Carlo simulation (Hansen, 2012). A correspondence between a given excluded volume distance distribution function $p_{\rm excl}(r)$ of a nonspherical object and the excluded volume distance distribution for some size distribution of spheres $f(R)$ can be established from equation (8) using the expression of Glatter (1980) for the cross-term distance distribution function $p_x(r, a, R_i, R_j)$.

Consequently an approximation to $p_{\rm excl}(r)$ for a nonspherical object may be calculated using $p_{\rm excl}(r)$ for a size distribution of spheres.

For monodisperse spheres and low volume fractions ($\eta < 0.1$) the structure factor is dominated by the contribution from the excluded volume as $-\int p_{\rm struct}(r)\,{\rm d}r \simeq 3.3\eta \times \int p_{\rm excl}(r)\,{\rm d}r$ in this region (Hansen, 2011). Therefore the structure factor for the size distribution of spheres is expected to be a good approximation to the structure factor for a nonspherical object, at least for small deviations from spherical symmetry and low volume fractions.

The effective volume fraction $\eta_{\rm e}$ which should be used for the spherical size distribution will be given by the ratio of the area of the excluded volume of $p_{\rm excl}(r)$ for the object to the area of $p_{\rm excl}(r)$ for the spheres (equation 11), *i.e.*

$$\eta_{\rm e} \simeq \eta V_{\rm red}/V_{\rm red,s}, \tag{12}$$

where $V_{\rm red}$ is the reduced volume for the nonspherical object and $V_{\rm red,s}$ is the reduced volume for the spheres.

3. Results

3.1. Polydisperse spheres

For the purpose of presenting the concentration effects of polydisperse spheres in direct space, the structure factor for a Schultz size distribution of hard spheres was calculated using the exact result of Vrij (1979) as well as the most frequently used approximations, *i.e.* the decoupling approximation of Kotlarchyk & Chen (1983), the local monodisperse approx-

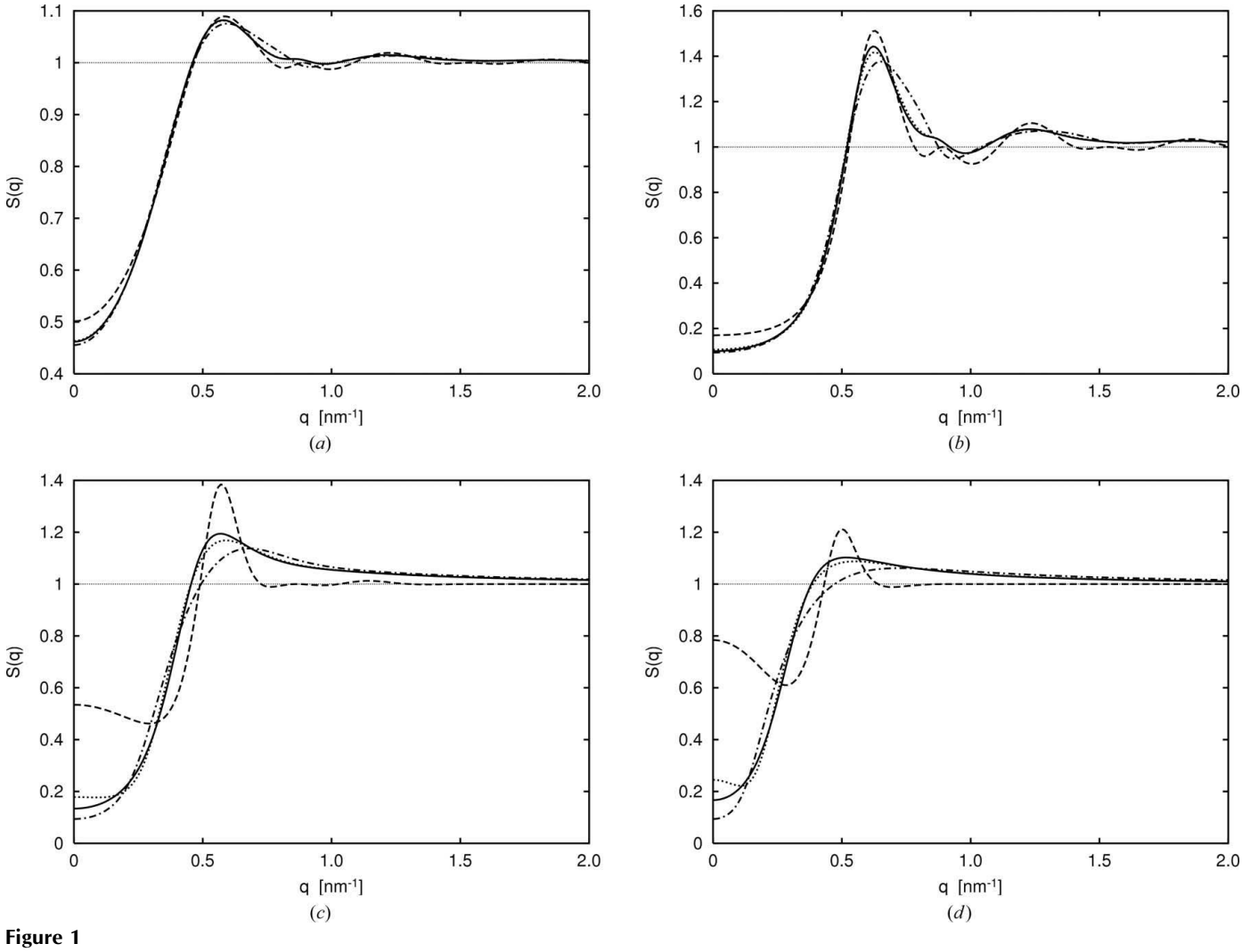

Figure 1
The structure factor $S(q)$ for a Schultz size distribution of spheres with $\langle R\rangle = 5$ nm. (*a*) $s = 0.1$, $\eta = 0.1$, (*b*) $s = 0.1$, $\eta = 0.3$, (*c*) $s = 0.3$, $\eta = 0.3$, (*d*) $s = 0.5$, $\eta = 0.3$. Solid lines: exact calculation (Vrij, 1979). Dashed: decoupling approximation (Kotlarchyk & Chen, 1983). Dashed–dotted: local monodisperse approximation (Pedersen, 1993). Dotted: scaling approximation (Gazzillo *et al.*, 1999).

imation of Pedersen (1993) and the scaling approximation of Gazzillo *et al.* (1999).

The Schultz size distribution of mean $\langle R\rangle$ may be defined by

$$f(R, \langle R\rangle, z) = \left(\frac{z+1}{\langle R\rangle}\right)^{z+1} R^z \exp\left[-\left(\frac{z+1}{\langle R\rangle}\right)R\right]\Big/\Gamma(z+1), \tag{13}$$

where Γ is the Gamma function and z is related to the relative width of the distribution, s, by

$$s = \frac{\sigma}{\langle R\rangle} = \frac{(\langle R^2\rangle - \langle R\rangle^2)^{1/2}}{\langle R\rangle} = (z+1)^{-1/2} \tag{14}$$

For small values of s the Schultz distribution tends toward a Gaussian of mean $\langle R\rangle$ and variance σ^2.

The structure factors for various volume fractions and widths of the size distribution are shown in Fig. 1. Using these structure factors with the respective form factors, the total intensities were calculated according to equation (2). The result is shown in Fig. 2. From these intensities the total distance distribution function $p_{\rm tot}(r)$ for each example was calculated using equation (3) and subsequently $p_{\rm tot}(r)$ was split into the different contributions according to equation (4). As both $p_1(r)$ and $p_{\rm excl}(r)$ can be calculated by integrations, $p_{\rm struct}(r)$ may finally be derived from $p_{\rm tot}(r)$ by simple subtractions as shown in Figs. 3 and 4.

The reduced molecular volume for a Schultz size distribution of spheres obtained using equation (10) is shown in Fig. 5(*a*).

3.2. Ellipsoids and cylinders

For a monodisperse solution the reduced molecular volume can be expressed analytically for many different molecular shapes (Ishihara, 1950), for example cylinders (Onsager, 1949) and ellipsoids of revolution (Ogston & Winzor, 1975). The reduced molecular volumes of cylinders and ellipsoids of revolution as a function of axial ratio are shown in Fig. 5(*b*).

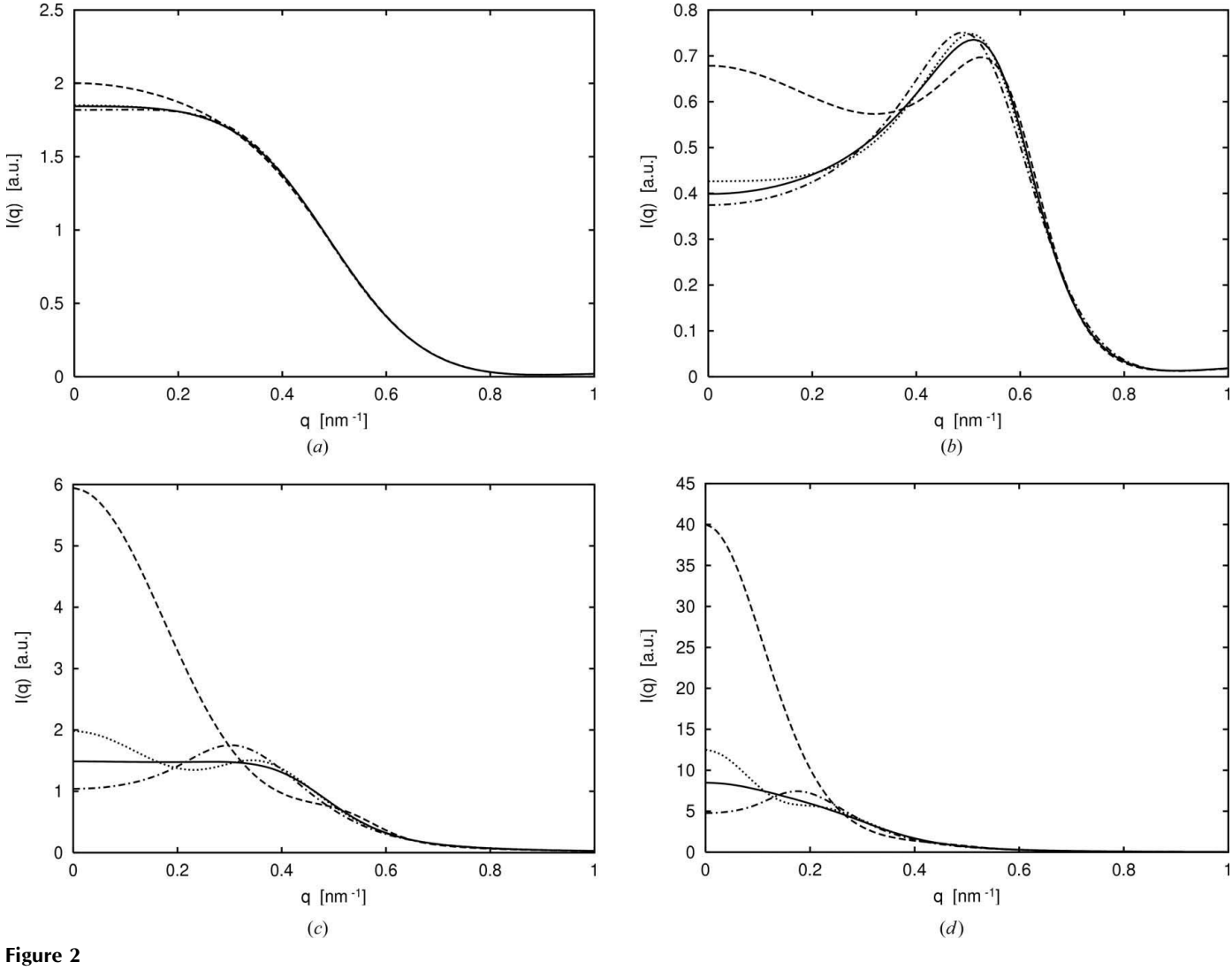

Figure 2
The scattered intensity $I(q)$ for a Schultz size distribution of spheres with $\langle R\rangle = 5$ nm. (*a*) $s = 0.1$, $\eta = 0.1$, (*b*) $s = 0.1$, $\eta = 0.3$, (*c*) $s = 0.3$, $\eta = 0.3$, (*d*) $s = 0.5$, $\eta = 0.3$. Solid lines: exact calculation (Vrij, 1979). Dashed: decoupling approximation (Kotlarchyk & Chen, 1983). Dashed–dotted: local monodisperse approximation (Pedersen, 1993). Dotted: scaling approximation (Gazzillo *et al.*, 1999).

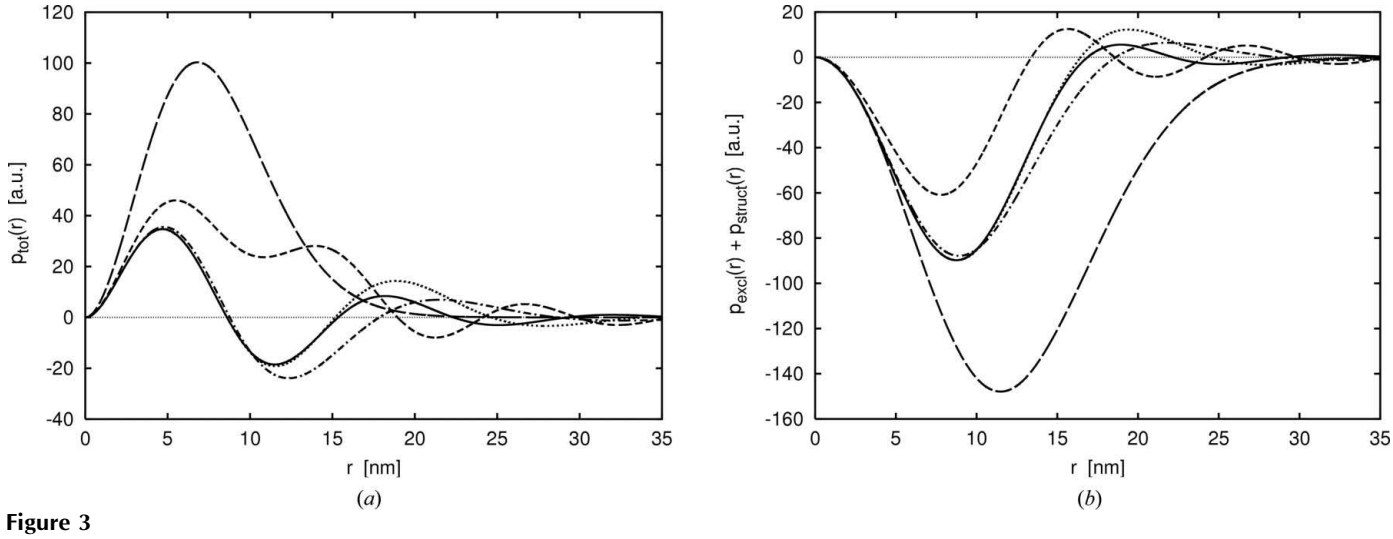

Figure 3
Distance distribution functions for a Schultz size distribution of spheres, having $\langle R\rangle = 5$ nm, $s = 0.3$ and $\eta = 0.3$ corresponding to Fig. 1(*c*). (*a*) $p_{\rm tot}(r)$, except long-dashed line which shows $p_1(r)$. Solid line: exact. Dashed line: decoupling approximation. Dashed–dotted: local monodisperse approximation. Dotted: scaling approximation. (*b*) $p_{\rm excl}(r) + p_{\rm struct}(r)$ calculated from (*a*) by subtraction of $p_1(r)$. Notation as in (*a*) except for long-dashed line which shows $p_{\rm excl}(r)$ calculated from equation (8).

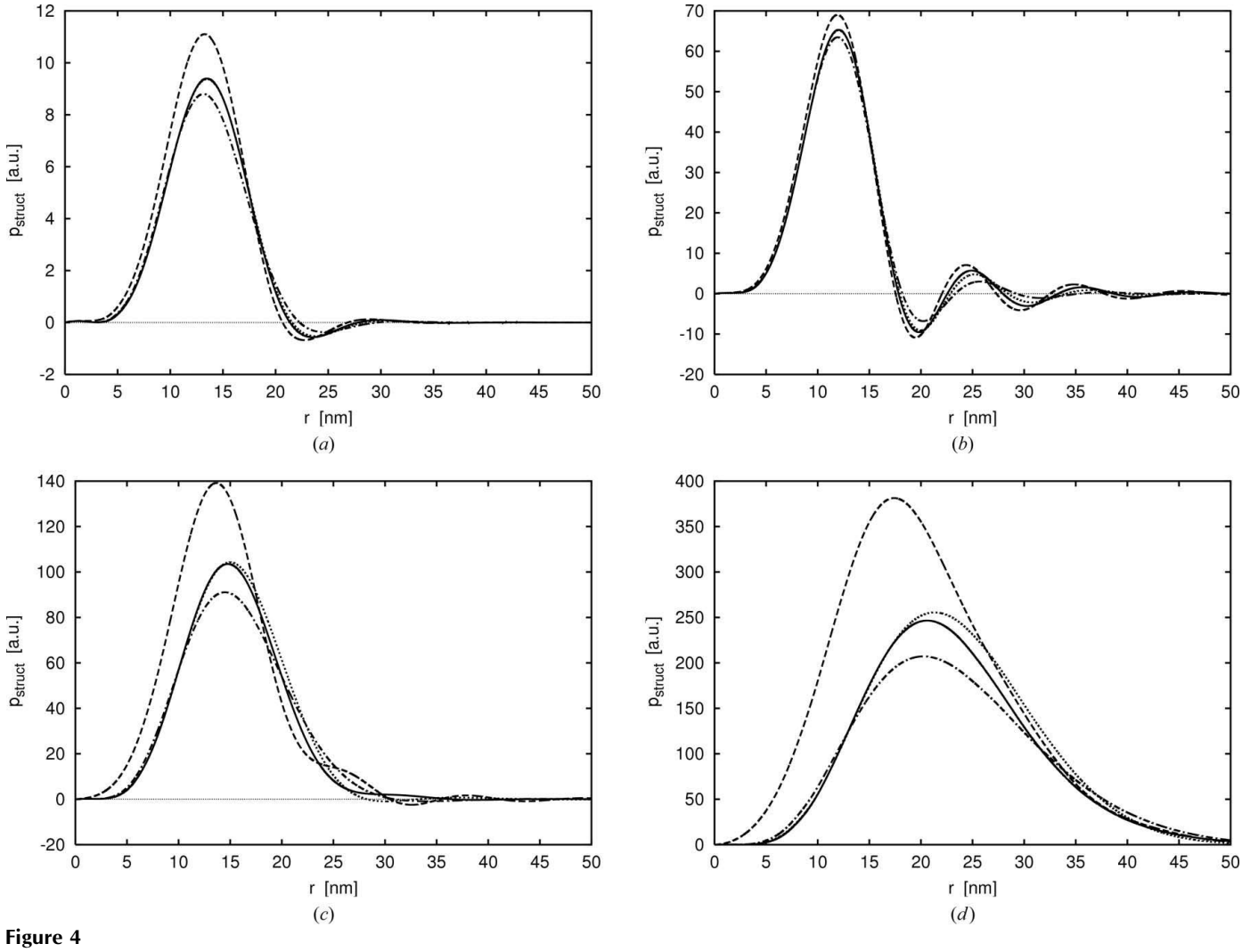

Figure 4
$p_{\rm struct}(r)$ corresponding to the examples shown in Fig. 1, calculated by subtraction of $p_{\rm excl}(r)$ from $p_{\rm excl}(r) + p_{\rm struct}(r)$. (*a*) $s = 0.1$, $\eta = 0.1$, (*b*) $s = 0.1$, $\eta = 0.3$, (*c*) $s = 0.3$, $\eta = 0.3$, (*d*) $s = 0.5$, $\eta = 0.3$. Solid lines: exact calculation. Dashed: decoupling approximation. Dashed–dotted: local monodisperse approximation. Dotted: scaling approximation.

The excluded volume distance distribution for a Schultz size distribution of spheres was used for fitting the excluded volume distance distributions of ellipsoids and cylinders of various axial ratios (calculated by Hansen, 2012). The Schultz distribution was chosen here because of its skewness for broad distributions compared to, for example, a Gaussian distribution. It was expected to give better agreement between the excluded volume distance distributions at longer distances where the excluded volume distance distributions for the cylinders or ellipsoids have a tail for large or small axial ratios.

In Fig. 6(*a*) is shown the average radius for a size distribution of spheres corresponding – with respect to their excluded volume distance distributions – to an ellipsoid of maximum diameter 2*a*. A similar result is also shown for cylinders of maximum length 2*a*. Fig. 6(*b*) shows the widths of the distributions.

For moderate axial ratios between 0.5 and 2.5 the difference between the excluded volume distance distributions of the ellipsoids/cylinders and those of the spheres was quite small. Denoting the maximum value for the excluded volume distance distribution function by $p_{\max}$, the absolute value of the distance between the points was typically less than $0.002p_{\max}$. To give examples of when discrepancies start to appear, Figs. 7(*a*) and 7(*b*) show the difference between the excluded volume distance distribution functions for ellipsoids of axial ratios 0.4 and 3.33, respectively, and the corresponding size distributions.

It should be noted that the spherical size distribution used for approximation of the structure factor is not equal to the spherical size distribution that gives a form factor equal to the form factor of the ellipsoid. This can be seen from Fig. 8, which shows the single-particle distance distribution function $p_1(r)$

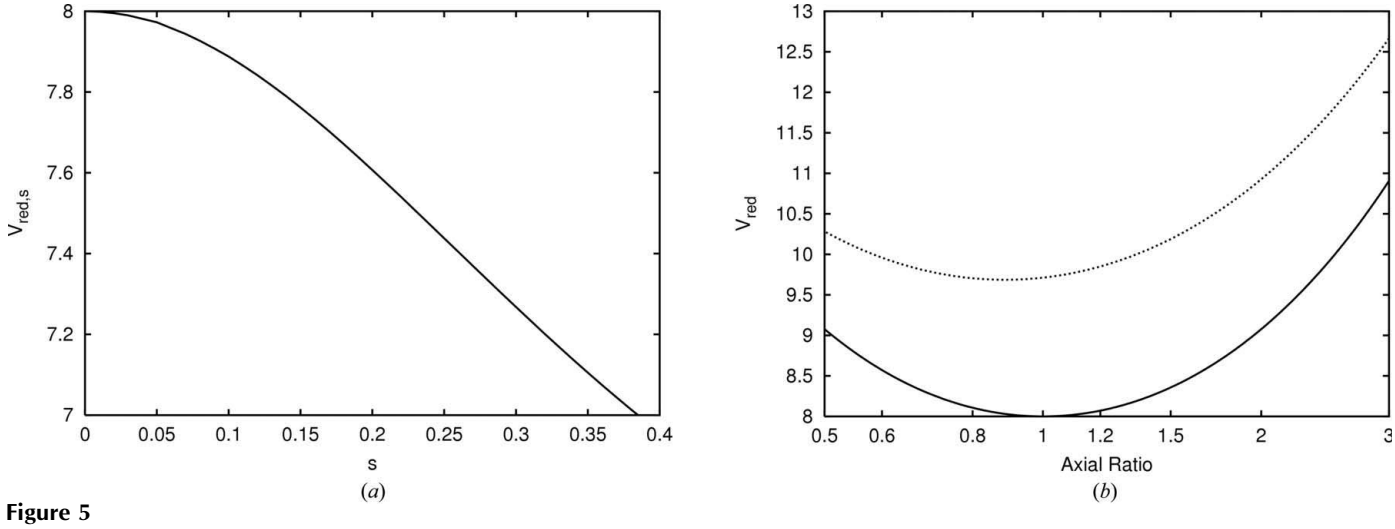

Figure 5
(*a*) The reduced volume for polydisperse spheres calculated from equation (10). (*b*) The reduced volumes for ellipsoids (solid line) and cylinders (dotted line) calculated following Ogston & Winzor (1975) and Onsager (1949).

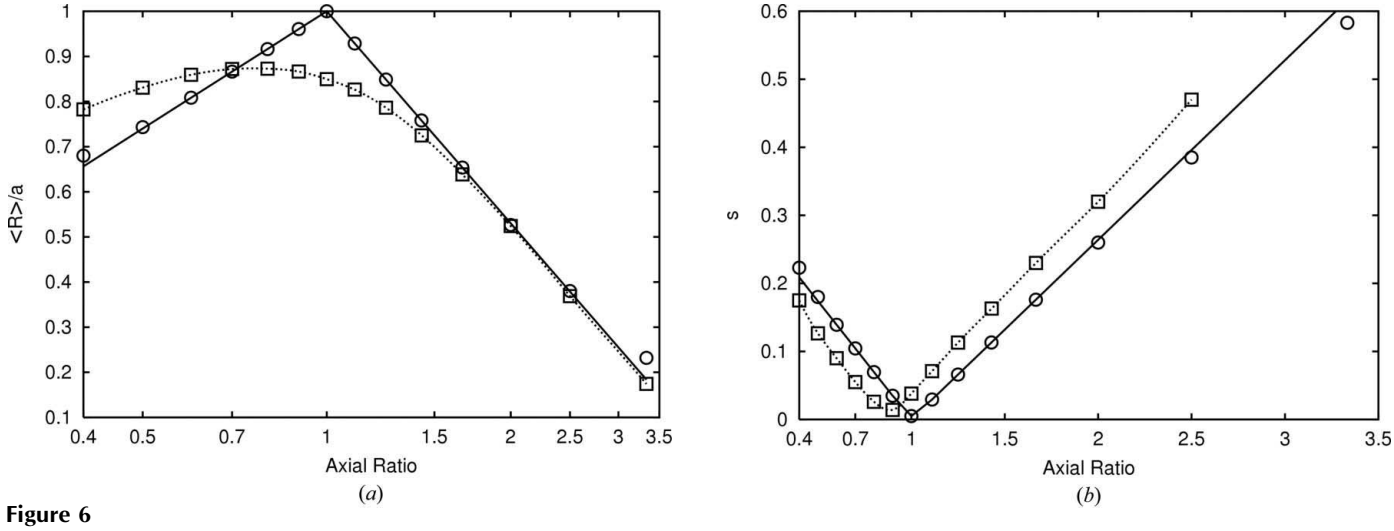

Figure 6
(*a*) The relative radius $\langle R\rangle/a$ for the spherical size distribution corresponding to the best fit between the excluded volume distance distribution of the spherical distribution and the excluded volume distance distribution of cylinders and ellipsoids (*a* is half the length of the cylinder or the maximum half-axis of the ellipsoid). Boxes: cylinders. Dotted line: spline fit. Circles: ellipsoids. Solid line: fit to ellipsoid data for small deviations from spherical symmetry [equations (15) and (17)]. (*b*) Width *s* of size distributions as in (*a*). Boxes connected by dotted line: cylinders. Circles: ellipsoids. Solid line: fit to ellipsoid data for small deviations from spherical shape [equations (16) and (18)].

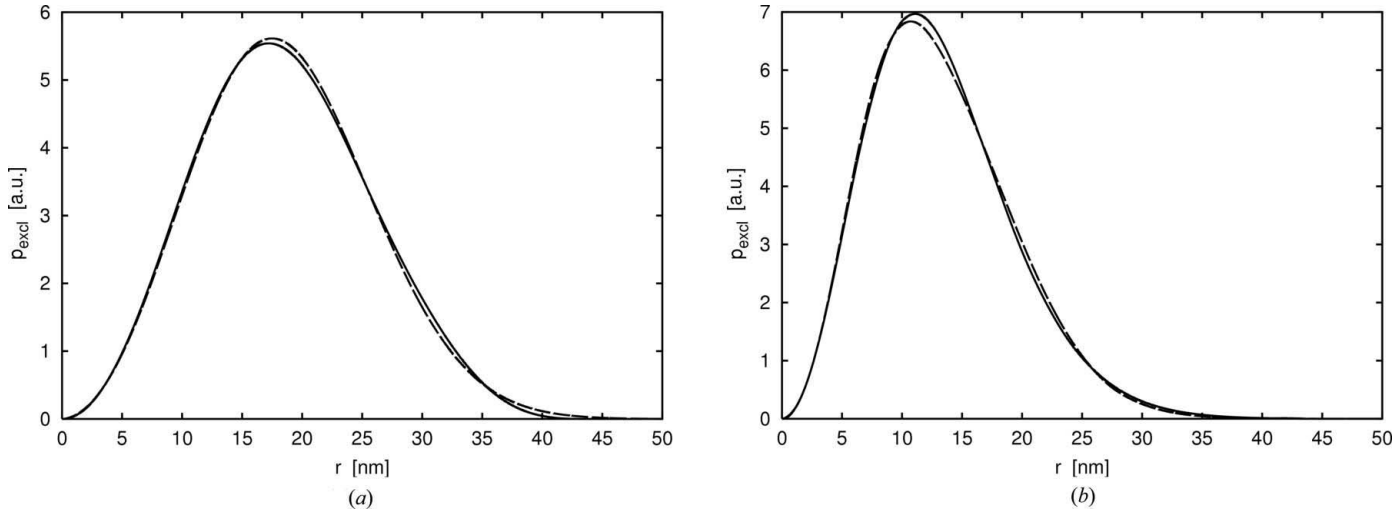

Figure 7
(*a*) The excluded volume distance distribution function $p_{\rm excl}(r)$. Long dashes: oblate ellipsoid, $a = 12.5$ nm and axial ratio $\varepsilon = 0.4$. Solid line: best fit with a Schultz size distribution of spheres. (*b*) $p_{\rm excl}(r)$. Long dashes: prolate ellipsoid, axial ratio $\varepsilon = 3.33$. Solid line: best fit with a Schultz size distribution of spheres.

for an ellipsoid of revolution of axial ratio 2.0 as well as $p_1(r)$ for a spherical size distribution giving the best fit of the excluded volume distance distribution of the ellipsoid (rescaled to give identical areas). In a corresponding plot of $p_{\rm excl}(r)$ the two curves are coinciding (not shown).

Fig. 9(*a*) shows the scattering intensities $I(q)$ from ellipsoids of revolution of axial ratio 2.0 and volume fraction 0.2 calculated using the decoupling approximation as well as using a Schultz size distribution of spheres having $\langle R\rangle = 6.62$ nm, $s = 0.264$ and $\eta = 0.246$ [parameters calculated using equations (15), (16) and (12), respectively]. Fig. 9(*b*) shows the corresponding $p_{\rm tot}(r)$ profiles obtained by Fourier transformation of the intensities. Figs. 9(*c*) and 9(*d*) show $p_{\rm excl}(r) + p_{\rm struct}(r)$ and $p_{\rm struct}(r)$ obtained by subtraction of the ellipsoidal $p_1(r)$ and $p_{\rm excl}(r)$, respectively. This makes it possible to express the differences between the two approximations as differences in their respective $p_{\rm struct}(r)$.

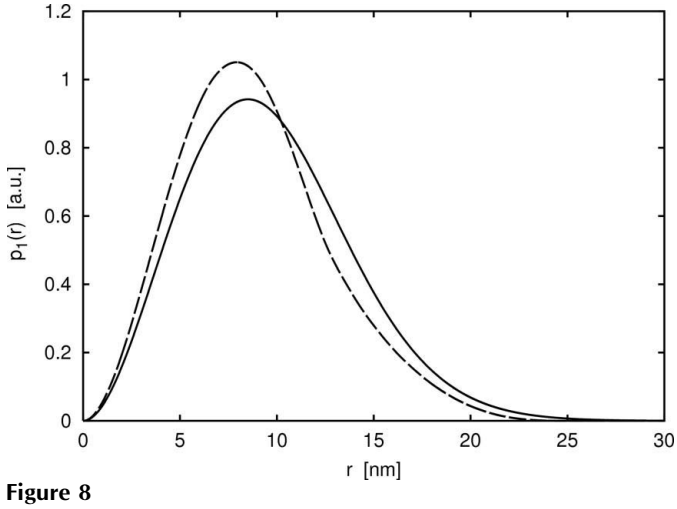

Figure 8
The single-particle distance distribution function $p_1(r)$. Solid line: Schultz size distribution of spheres with $\langle R\rangle = 6.62$ nm and $s = 0.264$. Long dashes: ellipsoid of revolution of $a = 12.5$ nm and axial ratio $\varepsilon = 2.0$.

3.3. Approximation for ellipsoids of moderate axial ratios

For ellipsoids of revolution of moderate axial ratios ($0.5 < \varepsilon < 2.0$) there appears to be a simple relation between the axial ratio and the average radius and polydispersity index s of the corresponding Schultz size distribution of spheres. In Fig. 6 this is shown in the form of linear fits to the calculations. As the scale in Fig. 6(*a*) is logarithmic this determines the expression for the average radius of the distribution,

$$\langle R(\varepsilon)\rangle = a\big[1 + c_R \ln(\varepsilon)\big], \tag{15}$$

and the widths of the size distribution can be written as

$$s(\varepsilon) = c_s(1 - \varepsilon), \tag{16}$$

with the parameters

$$c_R = \begin{cases} 0.375 & 0.5 \le \varepsilon < 1.0, \\ -0.678 & 1.0 \le \varepsilon \le 2.0, \end{cases} \tag{17}$$

and

$$c_s = \begin{cases} 0.348 & 0.5 \le \varepsilon < 1.0, \\ -0.264 & 1.0 \le \varepsilon \le 2.0. \end{cases} \tag{18}$$

Using these values for $0.5 \le \varepsilon \le 2.0$,

$$S_{\rm ell}(q, a, \varepsilon, \eta) \simeq S_{\rm sph}[q, \langle R(\varepsilon)\rangle, s(\varepsilon), \eta_{\rm e}]. \tag{19}$$

4. Discussion

From Figs. 1–4 it can be seen that it is possible to separate the contributions to the structure factor for polydisperse spheres into the different contributions from $p_1(r)$, $p_{\rm excl}(r)$ and $p_{\rm struct}(r)$ using the expression for the cross-term distance distribution of Glatter (1980).

From the form of $p_{\rm struct}(r)$ in Fig. 4 it is clear that the decoupling approximation suffers from an erroneous estimation of the excluded volume by allowing interference between particles at much too short distances. This is a consequence of the assumption of the decoupling approximation for polydisperse spheres: that the position and size of the spheres are uncorrelated.

The local monodisperse approximation gives a better estimate of the excluded volume at shorter distances, but contrary to the decoupling approximation the local monodisperse approximation implies structural interactions that are too weak, as can be seen from the relatively small area of $p_{\rm struct}(r)$. Consequently the forward scattering of this approximation is slightly too small.

For the scaling approximation a small overestimation of $p_{\rm struct}(r)$ at the largest distances only influences the innermost points in the scattering profile.

For ellipsoids, Fig. 6 indicates that small deviations from spherical symmetry lead to simple relationships for the parameters characterizing the corresponding size distribution. That this is not the case for cylinders is not surprising as an axial ratio of 1.0 does not coincide with the case of monodisperse spheres.

As the excluded volume distance distribution function contains information about the relative positions of interacting objects it may be expected that similarities in this function for two forms of objects may give similarities in their respective structure factors. However the structure factor is also dependent upon $p_1(r)$ and $p_{\rm struct}(r)$. Nevertheless, for small volume fractions where $p_{\rm excl}(r)$ dominates the contribution to the structure factor and for small deviations from spherical symmetry, the approximation suggested here appears more realistic than the decoupling approximation, which is based upon the nonphysical assumption that the positions and

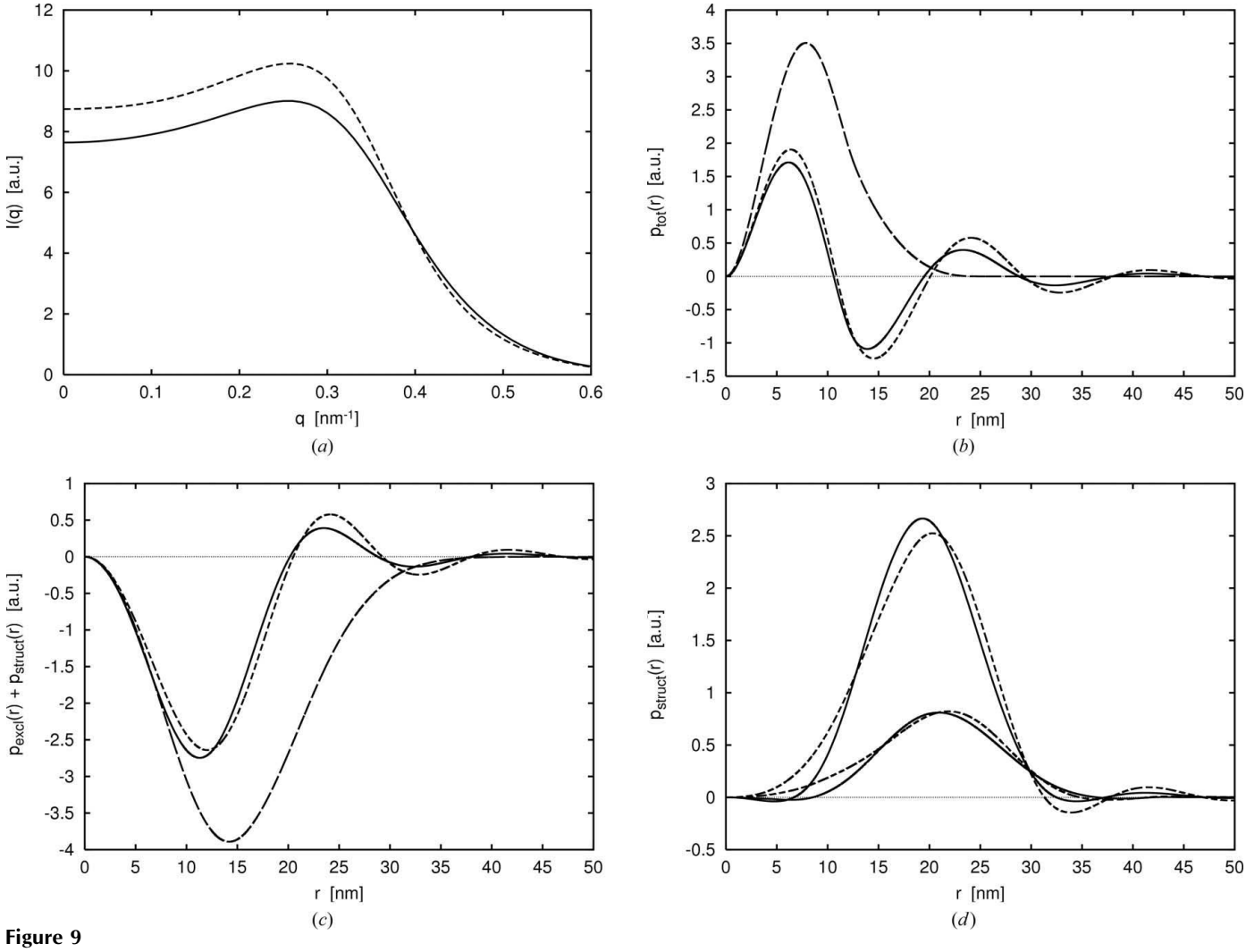

Figure 9
Comparison between the decoupling approximation and the spherical approximation for an ellipsoid of revolution of $a = 12.5$ nm, axial ratio $\varepsilon = 2.0$ and volume fraction $\eta = 0.2$. Dashed lines: decoupling approximation. Solid lines: approximation by a Schultz size distribution of spheres $\langle R\rangle = 6.62$ nm, $s = 0.264$ and $\eta_{\rm e} = 0.246$. (*a*) Intensities $I(q) = P(q)S(q)$. (*b*) $p_{\rm tot}(r) = p_1(r) + p_{\rm excl}(r) + p_{\rm struct}(r)$. Long-dashed line: $p_1(r)$ for the ellipsoid. (*c*) $p_{\rm excl}(r) + p_{\rm struct}(r)$ calculated by subtraction of $p_1(r)$ from $p_{\rm tot}(r)$. Long-dashed line: $p_{\rm excl}(r)$ from Hansen (2012). (*d*) $p_{\rm struct}(r)$ calculated by subtraction of $p_{\rm excl}(r)$. Upper two curves: $\eta = 0.2$. Lower two curves: $\eta = 0.1$.

orientations of interacting nonspherical particles are not correlated.

That this is the case is indicated in Fig. 9(*d*) where it can be seen that $p_{\rm struct}(r)$ calculated from the decoupling approximation for an ellipsoid of revolution of axial ratio 2.0 has a significant contribution at small distances where it should have been zero as in the corresponding distribution for spheres. Consequently the decoupling approximation will – similarly to the case for polydisperse spheres – again overestimate the intensity at small q values. Apparently the approximation by polydisperse spheres gives a more realistic estimate as $p_{\rm struct}(r) \simeq 0$ in the region approaching $r = 0$.

As the problem with the decoupling approximation is an erroneous estimation of the excluded volume contribution this makes it relatively more problematic to use the approximation at low volume fractions owing to the dominance of $p_{\rm excl}(r)$ in this region. This can also be seen from Fig. 9(*d*) where the relative difference between the two forms of approximations is larger for the low volume fraction (shown as the two lower curves). Fortunately the overall influence of the structure factor is lower at low volume fractions, which reduces the absolute value of the error of the decoupling approximation.

The results above were obtained using a simple Schultz size distribution characterized by only two parameters. Using a size distribution with more free parameters or even a free-form size distribution is likely to lead to better and more general results. Matching the sum of $p_{\rm excl}(r)$ and $p_1(r)$ of the two forms of objects instead of just $p_{\rm excl}(r)$ is also likely to improve the estimate.

5. Conclusion

For moderate deviations from spherical symmetry the structure factor for a nonspherical object may be approximated by the structure factor for a size distribution of spheres. The size distribution should be selected to give good agreement between the excluded volume distance distribution of the nonspherical particle and that of the size distribution of spheres. As the former may be calculated with good precision by Monte Carlo simulation and the latter is given by a semi-analytical expression it is possible to calculate the form of the size distribution giving the best agreement between the two excluded volume distance distribution functions. The results shown here indicate that this method may provide a better estimate of the structure factor for nonspherical particles than that of the frequently used decoupling approximation by including a more realistic estimate of the excluded volume. For ellipsoids of axial ratios between 0.5 and 2.0 the parameters of the corresponding size distribution have simple approximations which may be used, for example, for fitting purposes.

The Fortran source code used for this article is available from the author.

References

Cohen, A. P., Janai, E., Mogilko, E., Schofield, A. B. & Sloutskin, E. (2011). *Phys. Rev. Lett.* **107**, 238301.
Feigin, L. A. & Svergun, D. I. (1987). *Structure Analysis by Small-Angle X-ray and Neutron Scattering.* New York: Plenum.
Gazzillo, D., Giacometti, A., Valle, R. G. D., Venuti, E. & Carsughi, F. (1999). *J. Chem. Phys.* **111**, 7636–7645.
Glatter, O. (1980). *Acta Phys. Austr.* **52**, 243–256.
Glatter, O. & Kratky, O. (1982). Editors. *Small Angle X-ray Scattering*. London: Academic Press.
Hansen, S. (2011). *J. Appl. Cryst.* **44**, 265–271.
Hansen, S. (2012). *J. Appl. Cryst.* **45**, 381–388.
Ishihara, A. (1950). *J. Chem. Phys.* **18**, 1446–1449.
Kotlarchyk, M. & Chen, S.-H. (1983). *J. Chem. Phys.* **79**, 2461–2469.
Kruglov, T. (2005). *J. Appl. Cryst.* **38**, 716–720.
Mittelbach, P. & Porod, G. (1962). *Acta Phys. Austr.* **15**, 122–147.
Ogston, A. G. & Winzor, D. J. (1975). *J. Phys. Chem.* **79**, 2496–2500.
Onsager, L. (1949). *Ann. N. Y. Acad. Sci.* **51**, 627–659.
Pedersen, J. S. (1993). *Phys. Rev. B*, **47**, 657–665.
Pedersen, J. S. (1997). *Adv. Col. Int. Sci.* **70**, 171–210.
Percus, J. K. & Yevick, G. J. (1958). *Phys. Rev.* **110**, 1–13.
Svergun, D. I. & Koch, M. H. J. (2003). *Rep. Prog. Phys.* **66**, 1735–1782.
Vrij, A. (1979). *J. Chem. Phys.* **71**, 3267–3270.